SEDIMENT PRODUCTION AND DELIVERY FROM TIMBER HARVEST ROADS IN HUMBOLDT COUNTY, CALIFORNIA

By

Chris Faubion

A Thesis Presented to

The Faculty of Humboldt State University

In Partial Fulfillment of the Requirements for the Degree

Master of Science in Natural Resources: Forestry, Watershed, & Wildland Sciences

Committee Membership

Dr. Andrew Stubblefield, Committee Chair

Dr. Joe Wagenbrenner, Committee Member

Dr. Lee MacDonald, Committee Member

Dr. Kevin Boston, Committee Member

Dr. Erin Kelly, Graduate Coordinator

December 2020

ABSTRACT

SEDIMENT PRODUCTION AND DELIVERY FROM TIMBER HARVEST ROADS IN HUMBOLDT COUNTY, CALIFORNIA

Chris Paul Faubion

Sediment delivery from unpaved actively-used and relatively un-trafficked forest roads are one of the most common sources of impairment to aquatic ecosystems. Hence the objectives of this study were to: 1) compare the variability in erosion rates from actively used and relatively un-trafficked timber harvest roads across multiple water years in Railroad Gulch; 2) identify segment scale controls on road surface erosion and road-to-stream connectivity; 3) develop storm-based and annual segment scale models to predict road sediment production and compare the accuracy of these models to WEPP: Road; and 4) estimate road-related sediment loads to streams.

Between 2014 and 2019 mean plume lengths were four meters for active roads and two meters for inactive roads, whereas mean rill lengths were three meters on inactive roads and two meters on active roads. Only plume deposition proved significantly greater ($\alpha < 0.01$) on active roads compared to inactive roads.

The annual-based multiple regression model over-predicted sediment production by 28 percent and the storm-based underpredicted by 37 percent. WEPP: Road underestimated annual sediment loads by 95 percent. Segment-scale sediment production

is significantly correlated ($\alpha < 0.01$) to the slope*area of a road segment, increased rill length (m), percent bare soil, and summed storm erosivity (MJ mm ha^{-1} h^{-1}).

Sediment production rates for active and inactive roads in Railroad Gulch ranged from 0.0 kg m^2 yr^{-1} to 4.8 kg m^2 yr^{-1}. Since between one and two percent of active road lengths and between four and nine percent of inactive road lengths were connected between WY 2017 and 2019, an estimated five Mg and nine Mg of sediment would have delivered to the East and West Branch Railroad Gulch, respectively.

ACKNOWLEDGEMENTS

I would like to thank my wife Tara Cain-Faubion for her love and encouragement while I pursued this milestone in my life. I would not have been able to complete my thesis without the field support from my mischievous hound dogs Flora and Atlas, who always kept me company on long days while weighing buckets of sediment and walking brushy haul roads.

I am very appreciative to my advisor Dr. Andrew Stubblefield for the opportunity and wisdom offered throughout my time as a graduate student at Humboldt State University. I am also grateful for the thoughtful instruction and criticisms from my other committee members; Dr. Joe Wagenbrenner, Dr. Lee MacDonald, and Dr. Kevin Boston.

This thesis would not have been made possible without the financial support from CalFire. I would also like to thank Humboldt Redwood Company for allowing me to pursue this research on their property in the Lower South Fork Elk River. This thesis is evidence of their dedication to environmental stewardship and sustainable forest practices.

TABLE OF CONTENTS

LIST OF TABLES

LIST OF FIGURES

LIST OF APPENDICES

INTRODUCTION

Purpose

This project monitored the production of sediment from actively-used and relatively un-trafficked timber harvest roads in Railroad Gulch, a tributary to the lower South Fork Elk River in Humboldt County, California, USA (Figure 1). The data from this study evaluates the effectiveness of Humboldt Redwood Company's (HRC) best management practices (BMP's) for stormproofing timber harvest roads. Additional analysis has been conducted to develop and compare models for predicting sediment production from active and inactive roads located within the study area. The project is intended to fulfill HRC's Habitat Conservation Plan (HCP) for monitoring and evaluating the effectiveness of stormproofing roads for actual or potential occurrences of erosion, slippage, mass wasting, blocked or perched culverts, or any other sediment sources (HRC, 2014). HRC defines stormproofing as roads designed, constructed and maintained to minimize the delivery of fine sediment from roads and road drainage facilities to streams, as well as to minimize, to the extent feasible, sediment discharge to waters resulting from large magnitude storms and floods. Future land management decisions will benefit directly from a better understanding of sediment production and delivery from unpaved forest roads so that their impacts can be minimized.

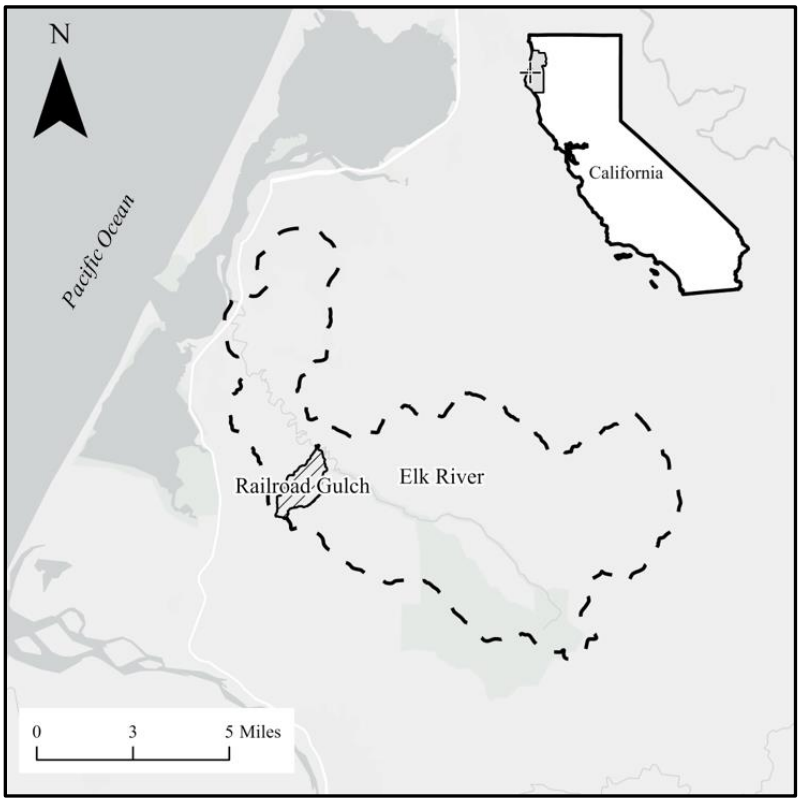

Figure 1. Location map of the Railroad Gulch watershed in Humboldt County, California.

Study Area and Objectives

Railroad Gulch consists of an East Branch (1.3 km^2) and a West Branch (1.5 km^2) and is a tributary to the lower South Fork Elk River in Humboldt County, California. Elevation ranges from 30 m to 335 m from the confluence of the East and West Branch to the uppermost point of the watershed. The lithology is comprised of Hookton and Wildcat formations. The Hookton is a Pleistocene era formation that consists of loosely consolidated sand and gravel, interfingered with blue-gray marine clay and silt (Evenson, 1959). The Wildcat series is a group of five formations ranging in age from Miocene to Pleistocene consisting of sandstone, marine siltstone, and claystone (Evenson, 1959). The

average annual precipitation for this region is 1024 mm which falls primarily from October 1st through May 31st (NOAA, 2018).

Both East and West Branches of Railroad Gulch were clear-cut in the early 1900's. The forest is currently comprised of dense third growth stands of conifers and hardwoods. Forest roads in both basins have been abandoned or closed to vehicle traffic since 2004. In 2015, HRC re-opened roads throughout the East Branch and constructed 0.8 km of new ridgetop road for timber harvest in the East Branch. In the summer of 2016 0.3 km^2 of forest were harvested using single tree selection and 0.2 km^2 were harvested using group selection. Roads in the West Branch were kept closed except for some light ATV traffic and 0.5 km of rocked haul road crossing through the lower part of the West Branch watershed. Roads throughout the East Branch received winter stormproofing following the installation of a ridge road in 2015 and the approval of the timber harvest plan in 2016.

Before the road construction in 2015 the road density was 8.8 km/km^2 in the East Branch, and after 2016 the active and inactive road densities were 6.2 km/km^2 and 2.6 km/km^2, respectively. Between 2014 and 2019 the West Branch of Railroad Gulch was left closed to vehicle traffic with an inactive road density of 6.8 km/km^2. Both East and West Branch Railroad Gulch were subject to light year-round ATV traffic by HRC staff as part of a paired watershed study to access monitoring stations throughout the catchment.

Between 2014 and 2019 a paired watershed study took place on the East and West Branch Railroad Gulch to monitor in-stream effectiveness and timber harvest plan (THP)

implementation. These two watersheds were selected because of similar geology, climate, topography, drainage networks, and the planned timber harvest on the East Branch of Railroad Gulch. A key part of this study included the assessment of road surface erosion and road-stream connectivity with a particular focus on the new road construction and effects of road use by logging equipment during timber harvest operations.

The objectives of this study were to: 1) compare the variability in erosion rates from actively used and relatively un-trafficked timber harvest roads across multiple water years in Railroad Gulch; 2) identify segment scale controls on road surface erosion and road-to-stream connectivity; 3) develop storm-based and annual segment scale models to predict road sediment production and compare the accuracy of these models to WEPP: Road; and 4) estimate road-related sediment loads to streams. Results from this study will aid in a better understanding of road related sediment production, as well as, inform resource managers when implementing BMP's to forest roads.

Background

Forest roads are critical to the timber harvest industry for resource extraction and forest management. However, the associated loading of fine sediment from forest roads into watercourses is known to degrade aquatic ecosystems (Suttle et al., 2004; Foltz et al., 2008). The combined transport of sediment to streams from forest roads and subsequent sedimentation transforms stream hydrology and reduces habitat suitability for aquatic species (Jones et al., 2000; Kolka and Smidt, 2004). The United States Environmental Protection Agency (EPA) lists sediment as the most common impairment to water quality

in streams and lakes in the United States (EPA, 2010). Land managers must understand forest road erosion processes to evaluate and limit the adverse impacts of forest roads on water quality and aquatic habitat.

Erosion rates from undisturbed forested hillslopes are typically very low due to high infiltration capacity as a result of the vegetative cover (Dunne and Leopold, 1978; MacDonald et al., 2003). In contrast, unpaved forest roads disturb the natural hillslope and are often devoid of vegetative cover and highly compacted with infiltration rates ≤ 5 mm hr^{-1} (Ziegler et al., 2007; Foltz et al., 2009; Ramos-Scharrón and LaFevor, 2016; Sosa-Pérez and MacDonald, 2017). Hence, erosion from forest roads is typically much higher than undisturbed forested hillslopes due to the lower rainfall intensities required for infiltration-excess (Horton) overland flow (HOF) to occur.

A range of erosion processes are associated with HOF. On the road surface, erosion takes place by rainsplash detachment, sheetwash, and rill erosion (Zeigler et al., 2000). When rainfall strikes the road surface it detaches smaller soil particles, and soil detachment from rainsplash is often 50 - 90 times greater than the detachment from surface runoff (Schwab et al., 1993). Both sheetwash erosion and rill erosion occur when the shear stress applied by the flow of water exceeds the resistance of the road surface (Dunne and Leopold, 1978; Luce and Black, 1999; Stafford, 2011). When surface runoff is concentrated into channels or tire ruts the road is more likely to develop rill erosion, which can dramatically increase sediment transport capacity and erosion rates (Elliot et al., 2009). The scale of these processes is also influenced by regional climate.

Local climate is important because this affects the magnitude, frequency, and duration of precipitation events (Ramos-Scharron and MacDonald, 2007). Precipitation at greater intensities often increases runoff and sediment production due to the larger drop sizes, increased rainsplash, and increase in HOF (Sugden and Woods, 2007). Studies published over the last two decades have reported annual road erosion rates per unit rainfall of 0.2 g m^{-2} mm^{-1} yr^{-1} to 10 g m^{-2} mm^{-1} yr^{-1} (Fu et al., 2010; Sosa-Pérez and MacDonald, 2017). The projected rise in rainfall intensities from climate change is likely to increase the rates of runoff and soil loss (Mullan et al., 2012).

In managed forest environments, there is a high degree of variability in the mechanisms generating the delivery of road runoff and sediment to a watercourse. Sediment from road sources is commonly delivered to streams at the outlet of a rill or gully, when a rill or sediment plume extends from a road drain to a channel, or when a road crosses a stream (Foltz et al., 2008). The effects of roads on water quality can be most efficiently reduced by identifying and treating only those road segments that deliver the greatest amount of sediment.

Best management practices outlined in the California Forest Practice Rules for reducing erosion rates and hydrologic connectivity include the following: (1) installation of a “disconnecting” drainage facility or structure close to the watercourse crossing; (2) increasing the frequency of ditch drain (relief) culvert spacing for roads with inside ditches; (3) converting crowned or insloped roads with inside ditches to outsloped roads with rolling dips; (4) removing or breaching outside berms on crowned or outsloped roads to facilitate crosswise drainage; (5) applying treatments to dissipate energy,

disperse flows, and minimize erosion at road drainage outlets not connected to watercourses; and (6) avoiding concentration of flows onto unstable areas (Brown et al., 2018). The recurring nature of sediment contributions from forest roads to streams indicates the importance of implementing BMP's for making informed land management decisions.

Tools for evaluating road surface runoff and erosion include, but are not limited to, road characteristic surveys, silt fences, monitoring precipitation and statistical models (Robichaud and Brown, 2002; Elliot et al., 2009). Silt fences are a versatile way to measure hillslope erosion and have a proven trap efficiency greater than 90 percent (Robichaud and Brown, 2002). The Water Erosion Prediction Project for roads (WEPP: Road) is one of the most commonly used erosion prediction models developed for estimating sediment production and delivery from unpaved forest roads (Elliot et al., 2009). This model includes the key characteristics that tend to control road sediment production, including climate, gradient, road area or length, road surface cover, soil texture, and traffic (MacDonald et al., 2003). Some key limitations to this model include no consideration of the role of rock armoring processes on sediment production, no consideration of mass wasting from cutslopes and fill slopes, and the need for better characterizing soils data for highly erodible road surfaces (Elliot et al., 2009).

METHODS

Precipitation

In summer 2017 a tipping-bucket rain gauge was installed with a resolution of 0.254 mm of rainfall per tip. The rain gauge was placed near the confluence of the East and West Branch of Railroad Gulch. Data from the rain gauge has been processed using the Revised Universal Soil Loss Equation (RUSLE) output from the USDA Rainfall Intensity Summarization Tool (RIST) to determine storm-by-storm summary of total precipitation depth (mm), duration (h), maximum 30 min intensity (I_{30}) in mm h^{-1}, and storm erosivity (EI_{30}) in MJ mm ha^{-1} h^{-1} (USDA, 2017). Storms were defined as periods with at least 1 mm of precipitation separated by periods of at least 60 minutes with no precipitation. Additional annual precipitation data for water years (WY) 2014 - 2019 were collected from the NOAA weather station on Woodley Island approximately 15 km to the Northwest in Eureka, CA.

Road Segment Characteristics

Detailed road segment surveys were conducted for 6.2 km of active roads and 2.3 km of inactive roads, and these were repeated for each summer from 2014 to 2018 (Appendix A). The surveys identified hydrologically distinct road segments, where a break between road segments was defined by road drainage features such as waterbars, rolling dips, or critical dips / culverts, or a stream crossing. The width and length of each road segment was measured using a 100-meter tape. Total road width was considered the

edge-to-edge distance across the entire road, while active road width was the distance across the portion of the road that was being driven upon. Slope was measured with a clinometer. Road surface type was considered rocked, native, or mixed. Percent vegetation and bare soil were recorded as ocular estimates. Cut and fill slopes were measured for their length, width, observed vegetative cover, and percent slope.

Road segments were classified into four main types: 1) outsloped, 2) insloped, 3) crowned, and 4) roughly flat. Outsloped roads drained runoff towards the outside or downhill edge of the road segment. Insloped roads drained runoff towards the hillside edge of the road segment, and were commonly designed with an inboard ditch with periodic relief from a cross draining culvert. Crowned road segments drained both to the outside and to the inside edge of the road segment. Crowned roads were rare in this study, and commonly had inboard ditches associated with their drainage features. Roughly flat road segments were typically constrained by through cuts or fill berms that directed surface flow downslope towards their drainage features (i.e., waterbars, rolling dips, or critical dips).

Road Erosion Information

Erosion information identified any drainage rill or sediment plume on or below a road segment, as well as, their potential to connect to a watercourse (Figure 2). Sediment plumes were measured for their length and width. Drainage rills were measured for their slope, width, length, and average depth. The roughness for each plume was sorted into four groups: 1) mostly smooth, 2) litter or small debris, 3) some blockages, and 4)

multiple large obstructions (logs, rocks, or deep chips). Cutbank and fill slope failures were measured for their approximate length, height, and depth.

Figure 2. Measuring plume deposition below a waterbar (a), and rill/gully erosion on an inactive road segment (b).

Road segments and their erosion features were also put into four connectivity classes. Segments with a connectivity score of one had no erosional features, while a connectivity score of four indicated that the erosion feature reached from the road to a watercourse. A road segment connectivity score of two signified that the cumulative length of erosion features (i.e., rill and/or plume) was less than 10 meters and did not connect to a watercourse. If a score of three was recorded then the cumulative length of erosional features was greater than 10 meters, and did not connect to a watercourse.

Road Sediment Production

Sediment production was measured from 27 road segments for water year 2018 and 2019 using silt fences (Figure 3) (Robichaud and Brown, 2002). Each fenced segment was randomly selected from three stratified slope classes of 0-5 percent, 6-11 percent, and >12 percent. Eighteen fences were placed on active haul roads with six replicates per slope class and nine fences were placed on inactive roads with three replicates per slope class.

Road condition surveys identified the characteristics of each road segment draining towards a silt fence (Appendix B). Precise measurements of surface cover were taken by 100-point counts on a zig-zag transect running down the road segment within the active road width. Each point was classified as bare soil, vegetation, leaf litter, or rock (intermediate axis >1.0 cm) (Sosa-Pérez and MacDonald, 2017).

The fencing used was a geotextile fabric attached to 1.5-meter wooden stakes and placed parallel to the downslope drainage feature of the selected road segments (Figure 4). The bottom of the fenced area was also lined with the geo-textile material to facilitate the removal of the captured sediment. The edges to the fences were buried or secured with landscape staples to ensure sediment was not lost underneath or out the sides of the fences.

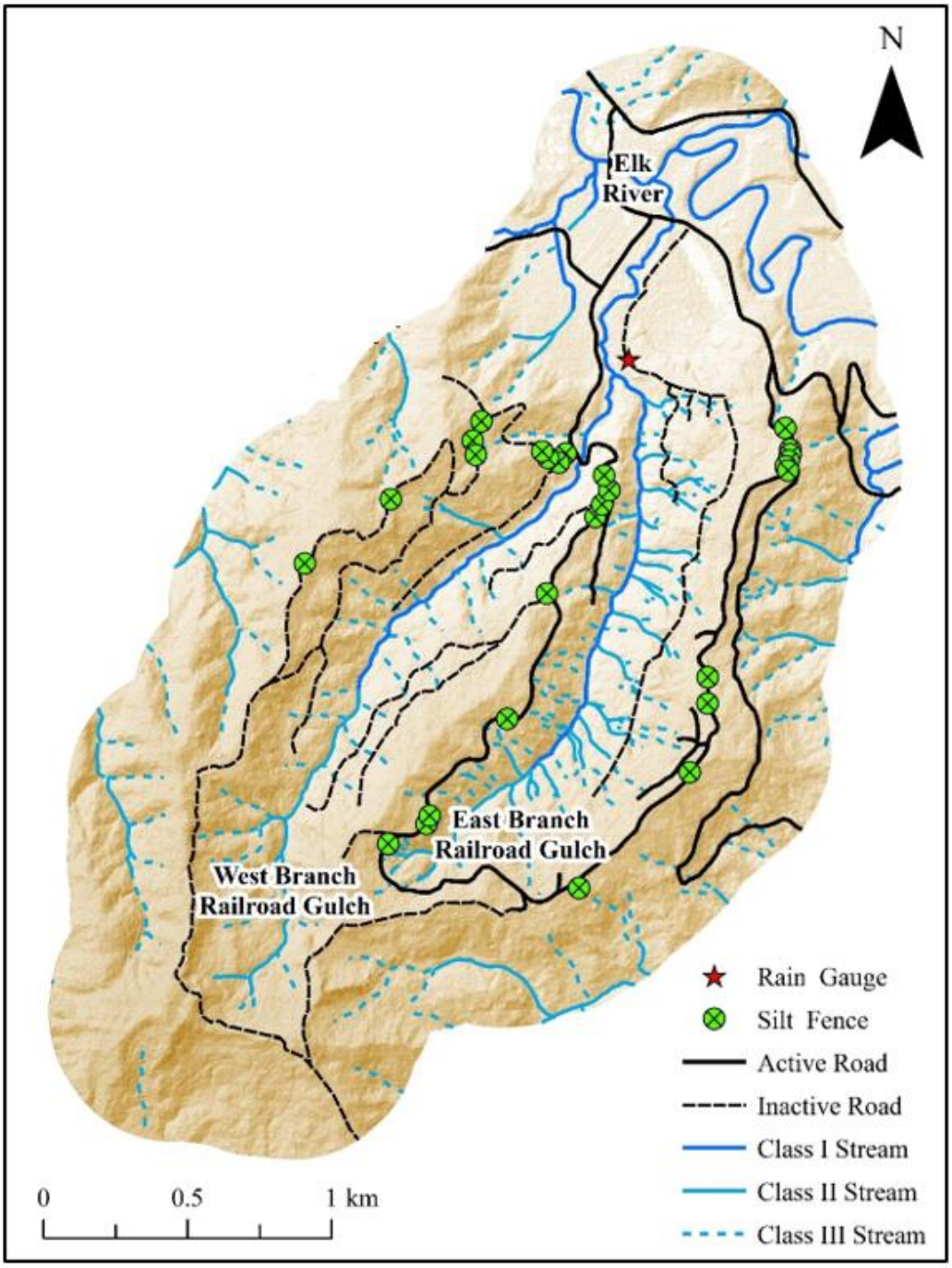

Figure 3. Map showing the Railroad Gulch watershed, active and inactive roads with silt fences, and the rain gauge below the confluence of the East and West Branch Railroad Gulch.

Figure 4. Silt fence on an inactive road segment with a slope class of 6-11 percent.

To the extent possible the mass of sediment captured in each fence was measured after each storm by shoveling the sediment into five-gallon buckets and weighing the samples with a 10 kg hanging scale to the nearest 0.1 kg. The measured wet weight of sediment was converted into a dry mass by weighing representative subsamples from each fence before and after drying for 24 hours at 105 ^{o}C (Topp and Ferré, 2002).

Statistical Analysis

Comparisons of road erosion features from active and inactive road surfaces were analyzed using a one-tailed paired sample Wilcoxon test with a selection criterion of $\alpha = 0.05$. This determined if road segment erosion features (i.e., plume lengths below drainages, plume lengths on road surfaces, or total road segment rill lengths) were significantly different between actively used and inactive roads in Railroad Gulch before and after road disturbance. Because it is a non-parametric test it does not require a normal distribution of residuals in the analysis (Cannon et. al., 2013).

Non-parametric Spearman correlation's and Kruskal-Wallis one-way analysis of variance were used to evaluate the univariate relationships between various road segment characteristics and erosion rates with a selection criterion of $\alpha = 0.05$ following Sosa-Pérez and MacDonald (2017). Covariates with significant univariate relationships were considered the dominant controls on erosion rates and were selected as part of a categorical decision tree (CART) to predict road-to-stream connectivity classes. A constructed categorical tree consists of nodes (each representing a road characteristic), branches (each representing the attribute value), and leaves (each representing a connectivity class) (Therneau and Atkinson, 2019). The model was cross validated by randomly selecting 70 percent of the data to train the model and the remaining 30 percent to test it.

Models for predicting road sediment production (kg yr^{-1}) on the segment scale for annual and storm-interval precipitation were created using multiple linear regression (Sosa-Pérez and MacDonald, 2017). The best-fit model was selected using criterion-based procedures in R Studio to formulate multiple combinations of the model's coefficients. Model outputs for R^2, Akaike Information Criterion (AIC) and delta AIC values were used to determine the best predictive model with a selection criterion for covariates of $\alpha = 0.05$ (Cannon et. al., 2013). AIC and dAIC are commonly used when comparing multiple models to evaluate the quality of each model relative to each other.

Estimating annual sediment production rates (kg yr^{-1}) were also preformed using WEPP: Road. WEPP: Road is a process-based model used to predicted road sediment production and delivery from road segment characteristics and climate data (Elliot et al.,

2009). The model is one of the most commonly used in forest practice throughout the United States. Model predictions for sediment leaving the road segment were based on covariates such as precipitation (mm), road gradient (%), road length and width (m), surface rock content (%), soil texture, and traffic level (Appendix C) (MacDonald et al., 2003). Precipitation data came from the Woodley Island weather station and soil type was set as silt loam.

Model Comparisons to WEPP: Road

Model comparisons were made through concordance analysis using a Bland-Altman diagram (Kwiecien et al., 2011). Where the average of measured and predicted values were plotted as the x-coordinate, and the difference between them as the y-coordinate. The mean of all differences was plotted as a solid horizontal line, with two additional horizontal lines plotted above and below at a distance of 1.96 times the standard deviation of the differences. Bland-Altman diagrams support a visual comparison of observed vs. measured data.

RESULTS

Precipitation

The average annual precipitation for this region is reported as 1024 mm which falls primarily from October 1st through May 31st (NOAA, 2018). Precipitation collected from the Woodley Island rain gauge in Eureka, CA ranged from 445 mm to 1577 mm for water years (WY) 2014 – 2019 (Figure 5). The driest WY was in 2014 with 445 mm of rainfall, while the wettest was 2017 with 1577 mm. In WY 2018 the confluence rain gauge produced 120 mm more precipitation than Woodley Island, and in 2019 155 mm.

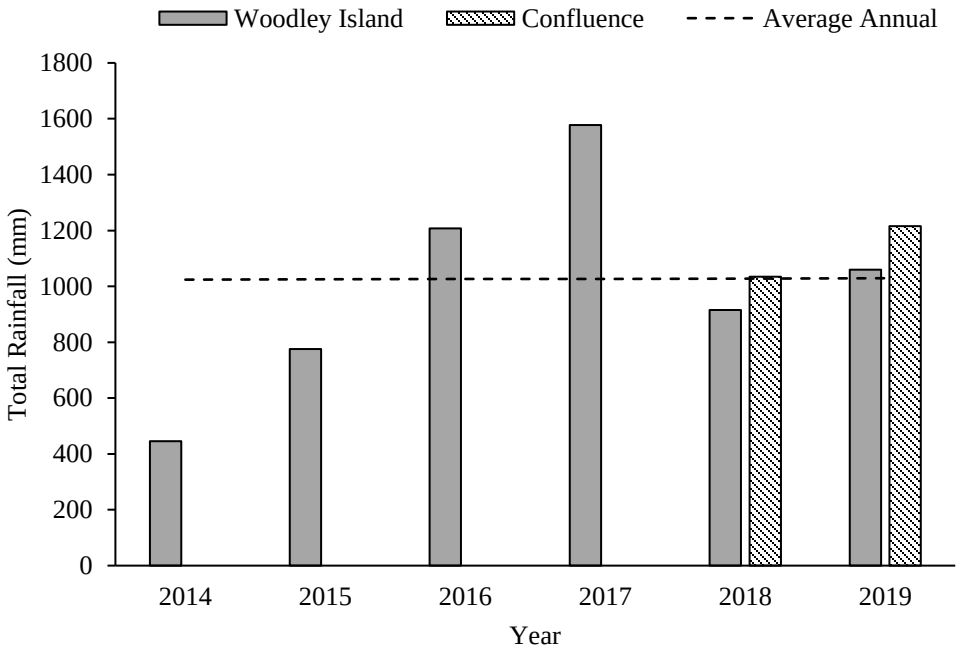

Figure 5. Annual precipitation from the rain gauge at Woodley Island in Eureka, CA. Dashed line represents mean annual rainfall.

Annual precipitation for the rain gauge at the confluence of Railroad Gulch was 6 percent higher than Woodley Island in WY 2018 and 20 percent higher in 2019. There were 113 storms with a total of 1035 mm of rain at the Railroad Gulch gauge in WY 2018, and 131 storms in 2019 with 1215 mm of rain. Roughly 70 percent of all storms were low intensity events with I_{30} values ranging from 0.1-5.0 mm hr^{-1} (Figure 6). Less than 10 percent of storms were greater than 10.1 mm h^{-1}.

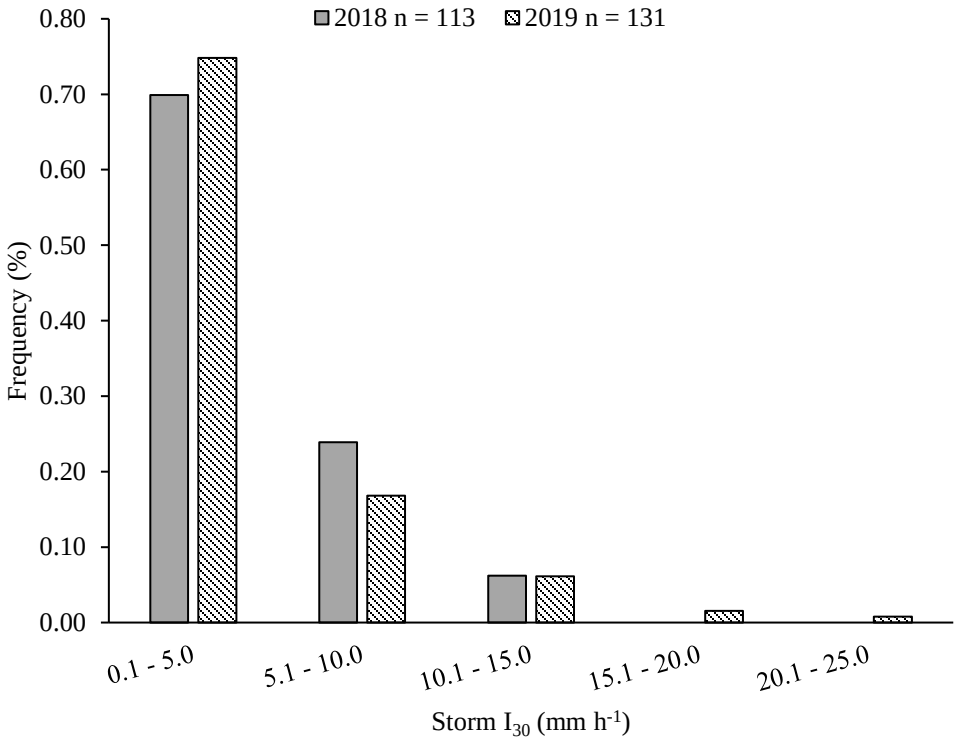

Figure 6. Frequency distribution of the maximum 30-minute rainfall intensity (I_{30}) for the 113 storms in 2018 and the 131 storms in 2019 from the rain gauge at the confluence of Railroad Gulch.

Road Segment Surveys

Road segment characteristics and erosion features throughout the East and West Branch varied across survey years. Prior to road installation and active use in 2014, 161 segments and four km of inactive road were surveyed in the East Branch of Railroad Gulch. Thereafter (2016-2019), 6.1 km of actively used road were surveyed which included 202 discrete road segments (Table 1). Inactive roads surveyed in the West Branch of Railroad Gulch were lightly used by ATV traffic and contained 84 road segments across 2.3 km during all years. Roads in both basins were not surveyed in 2015 due to lack of use and assumed similarity in conditions recorded in 2014.

Table 1. Mean road segment characteristics for survey years 2014-2019.

Road Segment Characteristic	**East Branch (2014)**	**East Branch (2016-2019)**	**West Branch (All Years)**
Total Survey Distance (km)	4.0	6.1	2.3
Total Number of Segments	161	202	84
Mean Segment Length (m)	25.6	28.5	27.7
Mean Total Rd Width (m)	3.5	5.7	3.0
Mean Cut Height (m)	1.8	1.3	1.7
Mean Rd Slope (%)	0.10	0.10	0.11
Mean Hill Slope (%)	0.22	0.24	0.29
Mean Bare Soil (%)	0.11	0.49	0.21
Road Drainage Type (%)	-	-	-
Critical Dip/culvert	0.06	0.03	0.04
Rolling Dip	0.37	0.20	0.21
Water Bar	0.58	0.76	0.71
Road Surface Type (%)	-	-	-
Rocked	0.06	0.17	0.00
Native	0.88	0.70	1.00
Mixed	0.05	0.13	0.00

Prior to road installation and timber harvest in 2014, the East Branch of Railroad Gulch consisted of mean road segment lengths equal to 25.6 m with total road widths averaging 3.5 m. After road installation in 2015, average road segment lengths and widths increased to 28.5 m and 5.7 m respectively. Mean cut bank heights on active roads after 2014 slightly decreased from 1.8 m to 1.3 m, due primarily to the addition of ridgetop road segments with lower and less frequent cut banks. Road segment slopes were consistent at 10 percent for all years on actively used roads, with hillslopes ranging from 22-24 percent.

Road drainage types and road surface types were dominated by water bars and native soil. Greater than 50 percent of all active and inactive road segments were drained by water bars, less than 40 percent were drained by rolling dips, and critical dips / culverts were associated with less than 10 percent of all segments. Inactive roads were not rocked and did not have mixed surface types. Dominant surface cover on inactive roads was vegetation or leaf litter. East Branch roads in 2014 had six percent of their road segments rocked with an additional 11 percent following active use from road installation and stormproofing in 2016.

The same inactive road segments in the West Branch Railroad were repeatedly measured each year, and therefore, had similar road segment characteristics throughout the study. Mean inactive road segment lengths and widths were 27.7 m and three m, respectively. Mean cut bank height was similar to active roads at 1.7 m. Road slopes for inactive roads averaged 11 percent, and hillslopes 29 percent.

The most notable difference in road segment characteristics prior to road installation and timber harvest were the change in percent bare soil (Figure 7). East Branch road segments in 2014 had an average of 11 percent bare soil then increased to 73 percent by 2016, and then to 78 percent in 2017. Percent bare soil on active roads following timber harvest declined to 34 percent by 2018, and then to 12 percent in 2019.

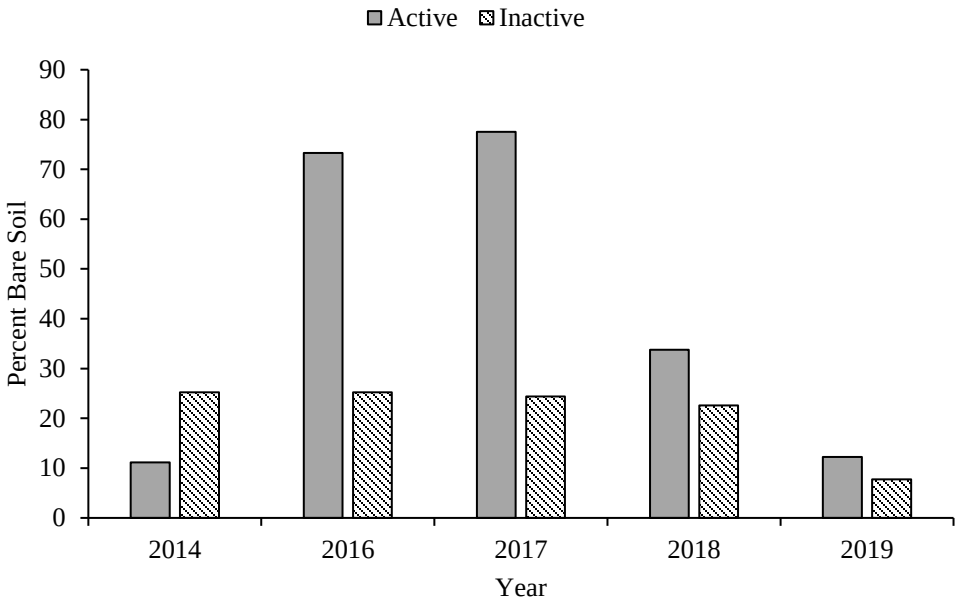

Figure 7. Percent bare soil on active and inactive road segments for years 2014-2019.

Inactive roads demonstrated lower percent bare soil compared to active road segments. Between years 2014-2018 percent bare soil on inactive road segments varied between 23 and 25 percent. However, by 2019 percent bare soil declined to eight percent, which was the lowest observed throughout the study and consistent with trends seen on active road segments.

Rill and plume features in the East and West Branch prior to disturbance (WY 2014) from road installation and timber harvest were very similar (Table 2). Mean rill lengths on road segments varied between basins by 0.5 m, and were not significantly different ($\alpha = 0.97$) in the one-tailed paired sample Wilcoxon test. Similarly, mean lengths of plumes on road surfaces varied by 0.2 m, and below segment drainages by 0.5 m and were not significantly different ($\alpha = 0.90$). This suggests that prior to 2016, roads in the East and West Branch Railroad Gulch had similar conditions in rill and plume feature lengths.

Table 2. Summary of rill and plume feature lengths for WY's 2014-2019 from the East and West Branch Railroad Gulch.

East Branch	Plume Length Below Drainage (m)	Plume Length on Road (m)	Rill on Road Length (m)
2014	1.7	0.0	0.1
2016	5.2	3.2	1.0
2017	6.4	5.0	2.0
2018	5.9	3.1	2.7
2019	5.9	3.1	2.8
West Branch	-	-	-
2014	2.2	0.2	0.6
2016	2.3	0.5	1.2
2017	2.5	0.3	1.2
2018	2.7	2.0	5.2
2019	2.7	2.0	5.6

Rill lengths were generally larger on inactive roads compared to active roads. Between 2014 and 2016 rilling on active roads increased from 0.1 m to 1.0 m, while inactive road rilling increased from 0.6 m to 1.2 m. By 2017, rilling on active roads increased from 1.0 m to 2.0 m, while inactive roads remained stable at 1.2 m. Interestingly, by 2018 inactive roads had increased rill lengths from 1.2 m to 5.2 m, while

active roads had only increased from 2.0 m to 2.7 m. In 2019, two years after timber harvest, rilling had again increased on active roads from 2.7 m to 2.8 m, whereas inactive roads had increased from 5.2 m to 5.6 m. Although inactive roads showed great increases in total rill lengths between 2014 and 2019, it was not significant in the paired samples Wilcoxon test ($\alpha = 0.43$) compared to rilling on active roads.

Seventeen percent of all road segments had rilling present between 2014 - 2019. Increased rill lengths on inactive roads were primarily the result of unmaintained rutting activity from ATV traffic, while rills on active roads were from both truck and ATV traffic. Limited rill length increases on active roads were the result of repeatedly being graded. Rilling in this study was minimal, but was strongly correlated to sediment plumes.

Post disturbances from road installation and timber harvest suggests evidence of increased plume lengths on active roads compared to inactive roads. Following road installation on active roads the mean plume length on road surfaces increased from 0.0 m to 3.2 m, which was significantly greater ($\alpha < 0.01$) than the corresponding increase on inactive road surfaces of 0.2 m to 0.5 m. In the same way, plume lengths below drainages increased from 1.7 m to 5.2 m on active roads, which was a significantly greater ($\alpha < 0.01$) increase compared to inactive roads of 2.2 m to 2.3 m.

Enlarged plume lengths following timber harvest were more subtle compared to increases following disturbances from road installation on active roads. Plume lengths on road segments increased from 3.2 m to 5.0 m by 2017, which was significantly greater ($\alpha < 0.01$) than the decrease of 0.5 m to 0.3 m on inactive roads. Likewise, plume lengths

below drainages on active roads increased from 5.2 m to 6.4 m, which was significantly greater ($\alpha < 0.01$) than the increase of 2.3 m to 2.5 m on inactive roads.

One and two years after timber harvest indicated a slight decrease then stabilization in mean plume lengths. By 2019 plume lengths on road surfaces and below drainages decreased to 3.1 m and 5.9 m, respectfully. Although plume lengths decreased in the two years following timber harvest, their mean lengths were still significantly greater ($\alpha < 0.01$) than those found on inactive roads.

Ninety-three percent of road segments with rills had plumes extend beyond their drainages. Plume lengths below drainages ranged from zero to 31 m long (Figure 8a). The presence of rilling on a road surface significantly increased ($\alpha < 0.01$) the mean length of travel for sediment plumes below their associated drainages by a factor of two. Alternatively, when roads were rocked the total rill and plume length of each segment was 1.9 times smaller, on average, compared to native road surfaces (Figure 8b). This decrease is significant in the paired samples Wilcoxon test ($\alpha < 0.01$). Reducing the distance that rill and plume features will travel from the road surface will ultimately lessen the likelihood of a road-to-stream connectivity.

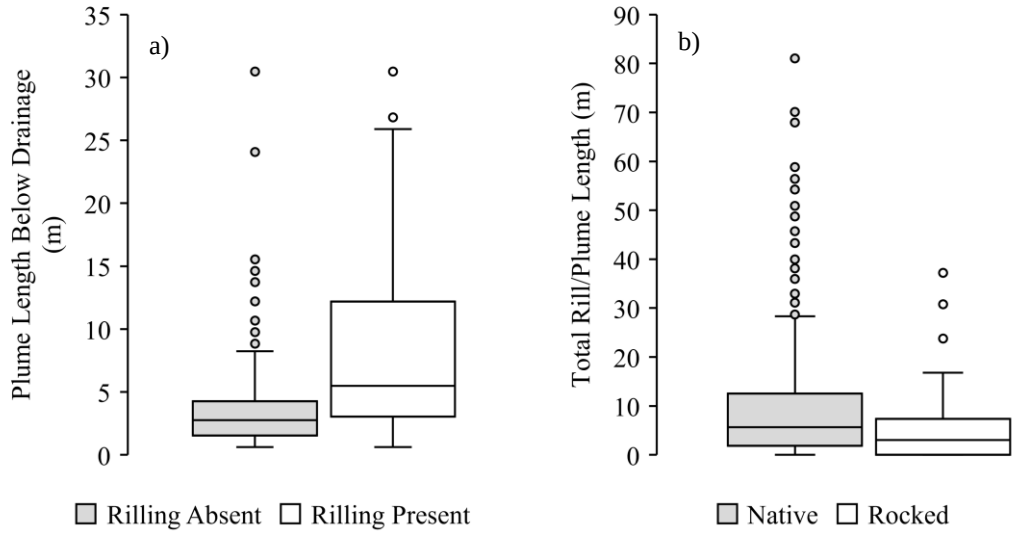

Figure 8. Box plot (a) shows the differences in plume lengths below drainages on road segments with rilling absent and present ($\alpha < 0.01$; n=215). Box plot (b) shows the differences in total rill and plume length on native vs. rocked road surfaces ($\alpha < 0.01$; n=1273)

Road-to-stream connectivity was greater on inactive roads compared to active roads. Between 2014 and 2019 the occurrence of greater than 10 meters of total rill and plume length on an active road segment increased from 2 percent to 43 percent, and from 8 percent to 32 percent on inactive road segments (Table 3). For active roads, the number of segments with no erosion dropped from 39 percent to eight percent, while inactive roads dropped from 31 percent to 18 percent.

Table 3. Percent of active and inactive road segments by connectivity class for each water year from 2014 to 2019.

Active Road	No Erosion	< 10 m Erosion	> 10 m Erosion	Connected
2014	39	60	2	0
2016	7	67	26	0
2017	5	42	51	2
2018	8	49	42	1
2019	8	48	43	1
Inactive Road	-	-	-	-
2014	31	61	8	0
2016	30	58	12	0
2017	30	52	14	4
2018	18	43	32	7
2019	18	43	32	7

Prior to 2017, a below average rainfall year, no road segments were connected to a stream. After 2017, an above normal precipitation year that followed timber harvest, there were four active road segments that were connected to a stream and three inactive road segments. By 2018, three active road segments and six inactive road segments delivered sediment to a watercourse. A one percent decrease in connectivity on active roads in 2018 was the result of a tree fall which diverted the previous year's plume connectivity away from the watercourse and onto the hillslope.

Connectivity from a road segment to a stream in the annual road surveys was associated with steeper hillslopes (>20 percent) and shorter distances to streams (<11 m). 40 percent of road segments that connected to a watercourse had rilling associated with their road surfaces. Additional road characteristics associated with road connectivity classes are shown in Table 4 and on the classification tree in Figure 9.

Table 4. Significance of correlation between road features and total measured length of rill and plume per road segment and the deviance explained by the Categorical and Regression Tree (CART) when predicting road connectivity class.

Road Feature	Kruskal-Wallis Test ($\alpha \leq 0.05$)	Spearman's Test ($\alpha \leq 0.05$)	Deviance Explained by CART (%)
Cut Bank Height (m)	-	0.01	1
Road Design (Inslope, Crown, Outslope, Flat)	< 0.01	-	3
Road Surface Type (Rock, Native, Mixed)	< 0.01	-	6
Road Area (m2)	-	< 0.01	25
Slope (%)	-	< 0.01	31
Bare Soil (%)	-	< 0.01	34
Drainage Ditch (Yes/No)	0.75	-	-

- indicates the model was not preformed because of the data type (i.e., continuous vs. categorical variables)

The classification tree indicates the breaks at maximum likelihood for characterizing the distribution of connectivity classes from active and inactive roads (Figure 9). All covariates were significant in the categorical decision tree following non-parametric Kruskal-Wallis tests for categorical variables and Spearman Correlation tests for continuous variables ($\alpha \leq 0.05$), with exception to the presence or absence of a drainage ditch ($\alpha = 0.75$) (Table 4). 70 percent of connectivity data was randomly selected to train the model and the remaining 30 percent was used to test it. The model accurately predicted connectivity classes 66 percent of the time when using the training data and 61 percent of the time when using the test data.

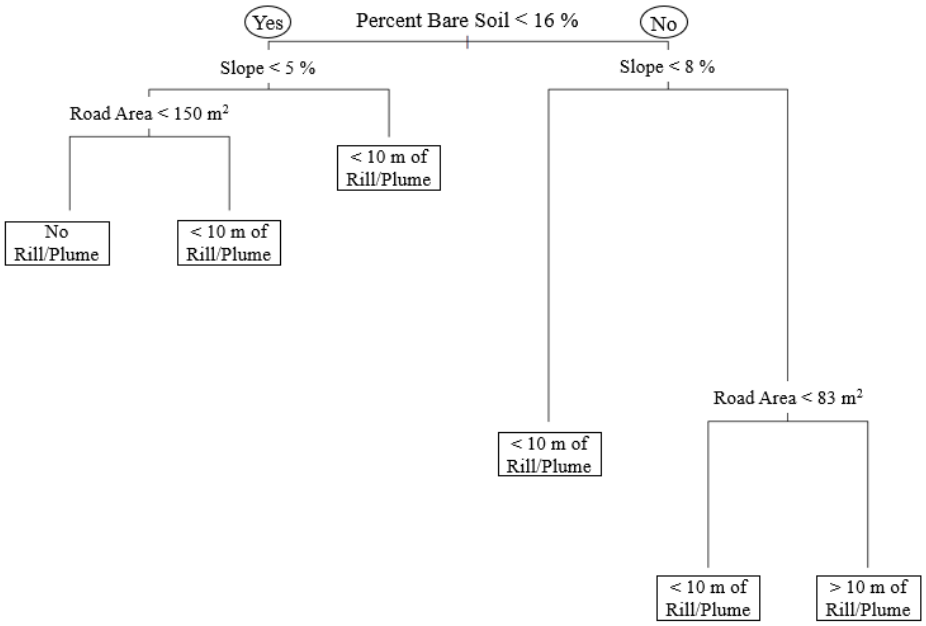

Figure 9. Categorical decision tree indicating segment characteristic controlling connectivity classes between 2014-2019 on active and inactive roads in Railroad Gulch.

Percent bare soil had the highest explained deviance in the model at 34 percent, followed by road slope at 31 percent, and road area (m^2) at 25 percent (Table 4). The least influential covariates were road surface type (rocked, native, or mixed), cut bank height (m), road design (crowned, inboard, outboard, or flat) and the presence or absence a drainage ditch. To achieve no erosion or deposition a road should consist of less than 16 percent bare soil with slopes below five percent, and a road area less than 150 m^2. When roads have greater than 16 percent bare soil, slopes above 8 percent, and road areas larger than 83 m^2 there will often be erosion features that exceed 10 m in length.

Road Segment Sediment Production

Silt Fence Road Segment Characteristics

Models for predicting road sediment production (kg yr^{-1}) on the segment scale for annual and storm-interval precipitation were created using multiple linear regression. Road segment characteristics and precipitation data were captured annually and used as covariates during model development. Storm-based regression models included sediment production values from grouped storm events, whereas annual models were developed from total sediment captured each year by silt fences. Model selection was criterion-based and used R^2, AIC, dAIC, and RMSE values as their performance metrics.

Active and inactive road segments chosen for silt fence installation were similar in their characteristics which allowed for reasonable comparison in this study (Table 5). The mean length of the 27 segments with a silt fence was 27.2 m on active roads and 29.4 m on inactive roads. Mean road width was 5.1 m on actively used roads and 2.6 m for the inactive roads. Mean cut bank heights between basins were less than one m of each other, and average slope was within half a percent. Both active and inactive road segment surfaces were un-rocked and comprised completely of native soil. Active roads had roughly twice as much bare soil as inactive roads, which is to be expected as active roads were graded and heavily trafficked during road installation and timber harvest. Between WY 2018 and 2019 percent bare soil on active and inactive roads dropped by nearly half due to decreased ATV traffic and increased cover from vegetation and leaf litter.

Table 5. Mean road segment characteristics and sediment production rates for silt fences installed on active and inactive roads. Values in parentheses are the standard deviations.

Road Segment Characteristic	**Active Roads**	**Inactive Roads**
Road Length (m)	27.2 (± 9.8)	29.4 (± 21.7)
Slope (%)	11.3 (± 7.1)	11.6 (± 7.6)
Active Width (m)	5.1 (± 0.2)	2.6 (± 1.3)
Cut Bank Height (m)	1.4 (± 1.0)	1.9 (± 3.0)
2018 Percent Bare Soil (%)	63.7 (± 28.3)	28.8 (± 25.0)
2019 Percent Bare Soil (%)	31.4 (± 18.2)	14.6 (± 13.7)
2018 Total Rill Length (m)	6.6 (± 10.9)	6.1 (± 9.4)
2019 Total Rill Length (m)	11.0 (± 15.6)	20.8 (± 29.8)
2018 Sediment Production (kg yr^{-1})	156.6 (± 199.7)	100.4 (± 190.3)
2019 Sediment Production (kg yr^{-1})	133.5 (± 191.9)	143.8 (± 221.6)

Between WY 2018 and 2019 sediment production decreased on active roads from 156.6 kg yr^{-1} to 133.5 kg yr^{-1}, whereas inactive roads increased from 100.4 kg yr^{-1} to 143.8 kg yr^{-1}. Alternatively, rilling between WY 2018 and 2019 on active roads increased from 6.6 m to 11.0 m, while inactive roads increased from 6.1 m to 20.8 m.

Annual-Based Road Sediment Production

Slope*area (SA), percent bare soil (BS), total rill length (RL), and cutbank height (CH) had the strongest association with $\log_e$ sediment yield (LSY) in kg yr^{-1} in the full equation (equation 1). Slope (SL), active road width (AW), road length (L), and road area (A) were comparable to SA, and therefore were not included in the full model as they are similar in function but have lower Pearson's correlation values to LSY (Table 6). Precipitation had no effect on LSY across WY 2018 and 2019 in the Pearson correlation plot, and therefore was removed from further analysis in the full annual-based model.

Table 6. Pearson correlations for coefficients used in multiple regression model for predicting annual-based sediment production.

	LSY	AI	SL	AW	L	A	SA	BS	RL	CH
LSY	-									
AI	0.26	-								
SL	0.74	0.04	-							
AW	0.44	0.83	0.23	-						
L	0.34	-0.08	0.21	0.00	-					
A	0.41	0.62	0.16	0.66	0.42	-				
SA	0.74	0.31	0.79	0.48	0.31	0.65	-			
BS	0.63	0.43	0.26	0.48	0.09	0.39	0.41	-		
RL	0.63	-0.13	0.63	0.11	0.59	0.10	0.50	0.16	-	
CH	0.49	0.00	0.61	0.10	0.38	-0.06	0.29	0.19	0.56	-
P	0.00	0.00	0.00	0.00	0.15	0.00	0.00	-0.46	0.23	0.05

*LSY is log sediment yield, AI is active/inactive road, SL is road slope, AW is active road width, L is road length, A is road area, SA is road slope * road area, BS is percent bare soil, RL is total rill length, CH is cutbank height, and P is precipitation.*

A natural log transformation of annual sediment yield was performed in order to meet the assumptions of the multiple linear regression model. Coefficients in equation 1 had variance inflation factors at or below 1.6, indicating nonexistent collinearity among covariates. The initial full model to predict LSY in equation 1 includes SA, BS, RL, CH, and whether the road segment was actively used or inactive (AI). Only SA, BS, and RL were significantly correlated ($\alpha < 0.01$) to LSY in the full multiple regression model.

$$LSY=\beta0 + \beta1(AI)+ \beta2(SA)+ \beta3(BS)+ \beta4(RL) + \beta5(CH) \quad \text{(equation 1)}$$

The results following the criterion-based tests for selecting a multiple linear regression using R Studio to run numerous combinations of models are shown in Table 7. The best annual-based model utilizes SA, BS, and RL to predict LSY, and this had a R^2 of 0.77 and a remarkably small RMSE of 2.2 kg. The Pearson correlations in Table 6 suggest that all coefficients are positively correlated with increased annual sediment

yield. The AIC for the three-parameter model was lower than the AIC for the one- and two-parameter models, and this also had a substantially higher R^2, a dAIC of 0.0, and the smallest RMSE. The F-statistic for the Annual C model is significant ($\alpha < 0.01$).

Table 7. Multiple regression models to predict annual-based sediment production with one, two, and three predictive variables, and the associated R2, AIC, dAIC, and RMSE.

Model	Equation	R^2	AIC	dAIC	RMSE
Annual A	LSY=β0 + β1(SA)	54.1	44.4	9.2	4.1
Annual B	LSY=β0 + β1(BS) + β2(RL)	68.0	39.6	4.3	2.9
Annual C	LSY= 0.05 + 0.08(SA) + 3.48(BS) + 0.05(RL)*	77.0	35.3	0.0	2.2

** indicates best fit model; LSY is log sediment yield, SA is road slope * road area, BS is percent bare soil, and RL is total rill length.*

Storm-Based Road Sediment Production

Storm-based models were developed using road segment surveys and rain gauge data from each year that the silt fences were installed. In total, six individual road segments were monitored each year which included 18 grouped storm events split evenly between WY's. Pearson's correlations in Table 8 indicates that slope*area (SA), percent bare soil (BS), total rill length (RL), and sum of storm erosivity (MJ mm ha^{-1} h^{-1}) ($\sum EI_{30}$) had the strongest correlation to storm sediment yield (SSY), and therefore were used in the full multiple regression model. Active and inactive roads (AI) did not affect the SSY and this variable was excluded from the model. The sum of maximum 30-minute rainfall intensities ($\sum I_{30}$) was dropped from the full model because it was substantially less correlated to SSY values than $\sum EI_{30}$.

Table 8. Pearson correlations for the variables used in the multiple regression models for predicting storm-based sediment production.

	SSY	**AI**	**SA**	**BS**	**RL**	**$\sum EI_{30}$**
SSY	-	-	-	-	-	-
AI	0.00	-	-	-	-	-
SA	0.47	-0.37	-	-	-	-
BS	0.18	-0.43	0.59	-	-	-
RL	0.28	0.44	0.12	-0.18	-	-
$\sum EI_{30}$	0.37	0.00	-0.07	-0.19	0.06	-
$\sum I_{30}$	0.18	0.00	-0.05	-0.13	0.04	0.70

*SSY is storm sediment yield (kg storm^{-1}), AI is active/inactive road, SA is road slope * road area, BS is percent bare soil (%), RL is total rill length (m), $\sum EI_{30}$ is the sum of storm erosivities within a sample time frame (MJ mm ha^{-1} h^{-1}), and $\sum I_{30}$ is the sum of maximum thirty-min storm intensities within a sample time frame (mm h^{-1}).*

A natural log transformation of storm sediment yield was performed in order to meet the assumptions of the multiple linear regression model. Coefficients in the model had variance inflation factors at or below 1.8, indicating nonexistent collinearity among the covariates. The full multiple regression model is shown in equation 2, where SA, BS, RL and $\sum EI_{30}$ were all significantly correlated ($\alpha < 0.01$) to $\log_e$ storm sediment yield (LSSY).

$$LSSY=\beta0 + \beta1(SA)+ \beta2(RL)+ \beta3(\sum EI_{30}) \qquad \text{(equation 2)}$$

The results following the criterion-based tests for selecting a multiple linear regression using R Studio to run numerous combinations of models are shown in Table 9. The best storm-based model utilizes SA, RL, and $\sum EI_{30}$ to predict LSSY, and this had a R^2 of 0.60 and a small RMSE of 1.6 kg. The Pearson correlations in Table 8 suggest that all coefficients are positively correlated with increased annual sediment yield. The AIC for the three-parameter model was lower than the AIC for the one- and two-parameter

models, and this also had a high R^2, a dAIC of 0.0, and a comparably small RMSE (Table 9). The F-statistic for the Storm B model is significant ($\alpha < 0.01$).

Table 9. Three top preforming multiple regression models to predict storm-based sediment production and their selection criterion.

Model	Equation	R2	AIC	dAIC	RMSE
Storm A	LSSY = β0 + β1(SA) + β2(RL)	0.52	34.1	0.2	1.9
Storm B	LSSY = -0.30 + 0.07(SA) + 0.02(RL) + 0.01($\sum EI_{30}$) *	0.60	33.9	0.0	1.6
Storm C	LSSY = β0 + β1(SA)+β2(BS)+ β3(RL)+ β4($\sum EI_{30}$)	0.63	35.0	1.7	1.5

** indicates the best fit model; LSSY is log_e storm sediment yield (kg storm^{-1}) SA is road slope * road area, BS is percent bare soil (%), RL is total rill length (m), and $\sum EI_{30}$ is the sum of storm erosivities within a sample time frame (MJ mm ha^{-1} h^{-1}).*

WEPP: Road Sediment Production

Table 10 suggest that road design, road gradient, road length, and average annual runoff are most strongly correlated with estimated annual sediment production leaving the road in the WEPP model. Average annual rain runoff (in) is calculated individually for each segment based on climate and road characteristics. Not represented in the table are road surface type, buffer length, and fraction of rock content, as these metrics were the same for all road segments and did not correlate to increased or decreased sediment production values in the final model. Similar to our results using regression models, many of the covariates were strongly correlated to annual sediment loads, however the WEPP model proved to greatly under predict sediment production rates by 95 percent.

Table 10. Pearson correlations for coefficients used in WEPP: Road model predicting annual-based sediment production.

	SLR	SLB	DSGN	RG	RL	RW	FG	FL	BGRD
SLR	-								
SLB	0.86	-							
DSGN	-0.42	-0.39	-						
RG	0.67	0.57	-0.54	-					
RL	0.72	0.61	-0.16	0.15	-				
RW	0.23	0.19	-0.04	0.23	-0.02	-			
FG	-0.05	0.24	0.12	0.04	-0.17	0.53	-		
FL	0.23	0.25	-0.02	0.01	0.23	0.60	0.52	-	
BGRD	0.39	0.38	-0.38	0.68	0.01	0.09	0.02	0.13	-
ARRO	0.80	0.85	-0.62	0.62	0.56	0.29	0.28	0.38	0.53

SLR is sediment leaving the road (kg yr^{-1}), SLB is sediment leaving buffer (kg yr^{-1}), DSGN is road design (outsloped rutted or outsloped unrutted), RG is road gradient (%), RL is road length (m), RW is road width (m), FG is fill gradient (%), FL is fill length (m), BGRD is buffer gradient (%), and ARRO is average annual rain runoff (in).

Model Comparison

In the Bland-Altman diagram the upper two lines correspond to the limits of agreement. The mean-of-all differences line indicates the systematic deviation of the measured vs. predicted values for the limits of agreement (LOA). The mean of all differences line should be close to zero indicating no systematic deviation between measured and predicted values. In addition, the majority of points should fall inside the upper and lower limits of agreement which indicate that the observed and predicted data fall within the 95 percent confidence interval.

The Annual C model overpredicted sediment production rates by 28 percent when compared to measured values. The Bland-Altman diagram confirms that the observed and measured values are in fairly close agreement with one outlier outside of the 95th percentile of the upper and lower LOA (Figure 10). The mean of all differences (Bias) is

the closest to zero compared to other models at 52.8 kg yr^{-1}. The differences between the two measurements will be less than 1087.7 kg yr^{-1} 95 percent of the time; this difference is high relative to the measured maximum value of 643.3 kg yr^{-1}.

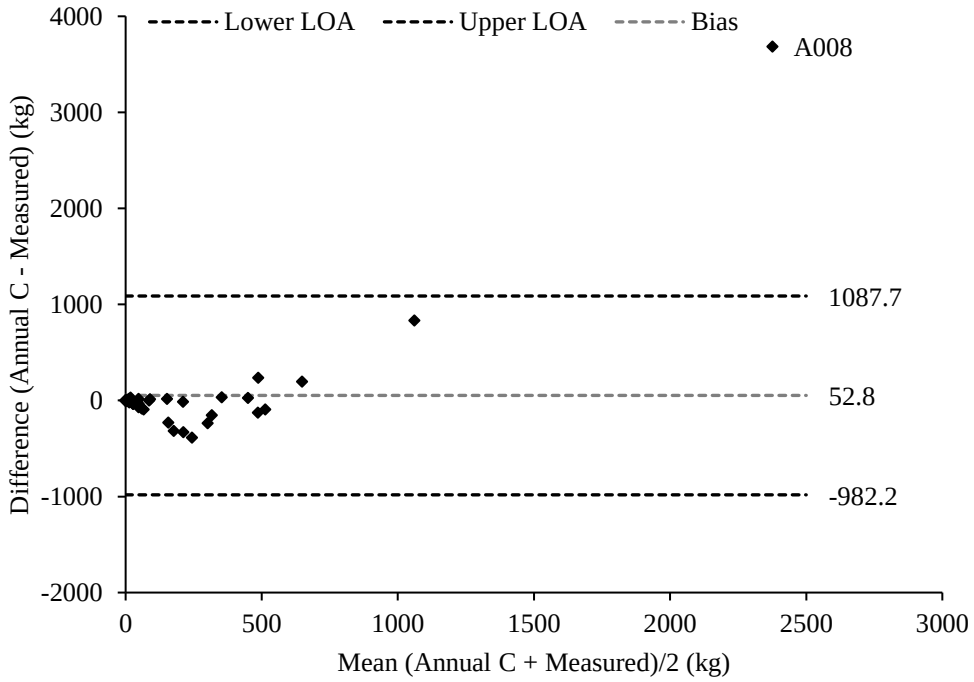

Figure 10. Bland-Altman diagram comparing measured vs. predicted values from the Annual C model (n = 54).

The Storm B model underpredicted sediment production rates by 37 percent when compared to measured values. The Bland-Altman diagram confirms that the observed and measured values are in close agreement with all estimates within the 95th percentile of the upper and lower LOA (Figure 11). The mean of all differences (Bias) is - 63.5 kg yr^{-1}. The differences between the two measurements will be less than 186.0 kg yr^{-1} 95 percent

of the time; this difference is low relative to the maximum measured value of 511.5 kg yr^{-1}. The diagram also suggests that the Storm-B model over predicts small events and under predicts large events.

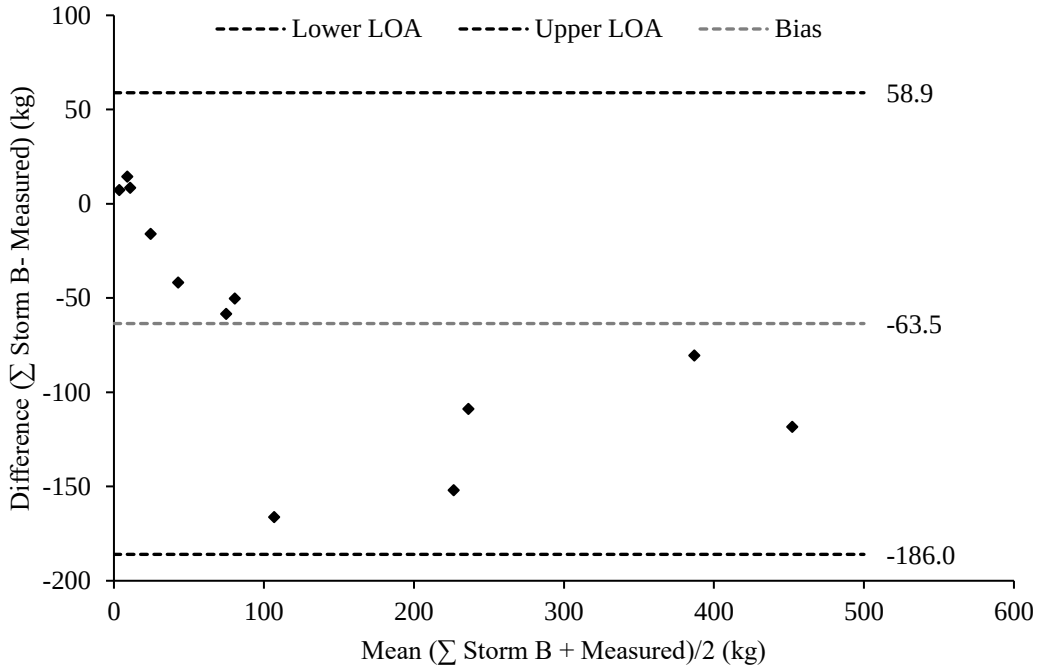

Figure 11. Bland-Altman diagram comparing measured vs. predicted values from the Storm B model (n = 12).

WEPP: Road underpredicted sediment production rates by 95 percent when compared to measured values. The Bland-Altman diagram confirms that the observed and measured values are in poor agreement with several estimates outside of the 95th percentile of the lower LOA (Figure 12). The WEPP mean of all differences (Bias) is farthest from zero at -130.6 kg compared to the Annual and Storm-based models. The differences between the two measurements will be less than 502.2 kg yr^{-1} 95 percent of the time; this difference is low to the measured maximum value of 643.3 kg yr^{-1}. The

diagram also shows a linear trend indicating that as measured values continue to increase the estimates from WEPP get gradually smaller.

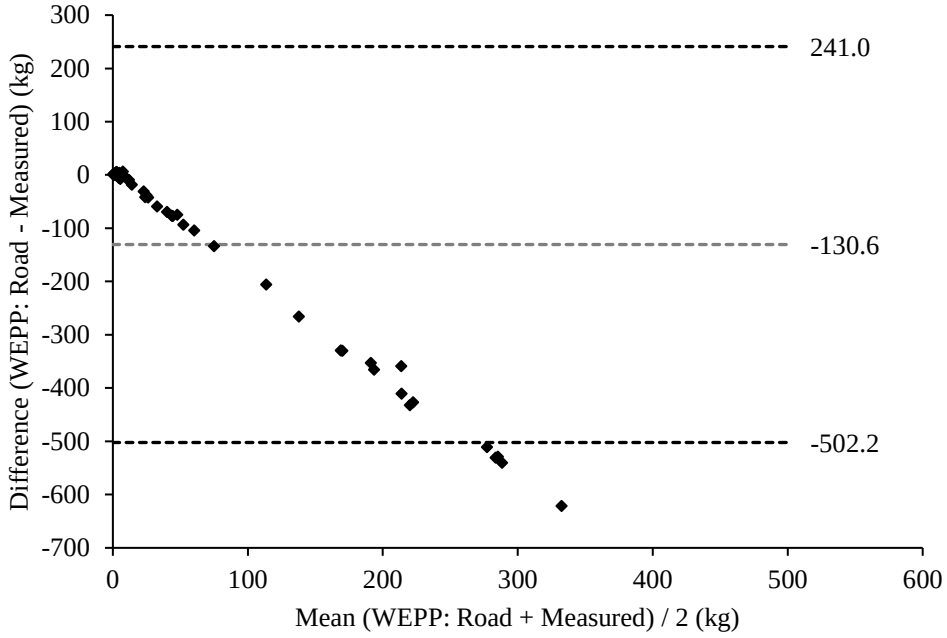

Figure 12. Bland-Altman diagram comparing measured vs. predicted values from the WEPP: Road model (n = 54).

Road-related Sediment Loads to Streams

A critical question for evaluating cumulative watershed impacts is how sediment production rates from actively used roads compare to the values from inactive roads. Between 2018 and 2019 field measurements of sediment production rates ranged from 0.0 kg m^2 yr^{-1} to 4.8 kg m^2 yr^{-1}. Over the two-year period the mean sediment production rate per unit rainfall for both active and inactive roads combined was 1.1 g m^{-2} mm^{-1} yr^{-1}. In 2018 the mean annual sediment production rate for active roads was 1.1 g m^{-2} mm^{-1} yr^{-1}, while inactive roads were 0.9 g m^{-2} mm^{-1} yr^{-1}. In 2019 mean annual sediment

production rates were 0.8 g m^{-2} mm^{-1} yr^{-1} for active roads, and 1.5 g m^{-2} mm^{-1} yr^{-1} from inactive roads. Covariates from field measurements in the annual and storm-based regression models suggest that the difference between years in sediment production rates is likely due to a decrease in bare soil on active roads from 63.7 percent to 31.4 percent, and an inactive road rill length increase of 6.1 m to 20.8 m.

Sediment production and delivery from active and inactive forest roads in Railroad Gulch can be estimated by multiplying the corresponding mean annual sediment production rate (g yr^{-1}) by total road area (m^2), precipitation depth (mm), and by the percent road length connected from WY's 2017-2019. The mean sediment production rate for active roads in Railroad Gulch is 1.0 g m^{-2} mm^{-1} yr^{-1} and inactive is 1.2 g m^{-2} mm^{-1} yr^{-1}. Since between one and two percent of active road lengths and between four and nine percent of inactive road lengths were connected between WY 2017 and 2019 an estimated five Mg and nine Mg of sediment would have delivered to the East and West Branch Railroad Gulch during those years combined, respectively. For comparison, this is less than one percent of the total measured load captured from sediment gauging stations on the lower East and West Branch of Railroad Gulch.

DISCUSSION

Sediment plumes and road surface rill lengths in this study were generally less than values reported elsewhere. The overall mean plume and rill length in this study was four m for active roads, and two m for inactive roads. Other researchers have found that the mean length for road-derived sediment plumes and outlet rills in Idaho averaged 11 m (Megahan and Ketcheson, 1996), 12 m in the Sierra Nevada (Coe, 2006), and 25 m in the Colorado front range (Welsch, 2008). Mean erosion feature lengths in Railroad Gulch were most similar to the mean length of five and nine m found for old and new roads on sandstone lithology in the Oregon Coast Range (Brake et al., 1997). Differences in climate, lithologies, vegetation, and road management strategies among studies likely played a large role in the differences in rill and plume feature lengths.

Rill lengths were generally larger on inactive roads compared to active roads in this study. The most substantial increase in rill lengths from 1.2 m to 5.6 m occurred on inactive roads following an above average precipitation year of 1035 mm in 2018. Previous years, 2014 - 2015 were below normal precipitation years (445 mm - 776 mm) and had marginal increases in rill length from 0.6 m to 1.2 m. Interestingly, 2017 was a particularly wet year (1577 mm) and yet rill lengths remain low at 1.2 m. One major difference is that 2018 was the fourth year of unmaintained rutting activity from ATV traffic following two years of previously above average precipitation. Increased rill lengths were mitigated on active roads by repeatedly being graded following road installation and timber harvest in 2015 and 2016.

In this study the presence of rilling on a road segment significantly ($\alpha < 0.01$) increased plume length below drainages by a factor of two. The greatest increase in plume lengths below drainages occurred on active roads following an above average precipitation year (1207 mm) and disturbance from road installation in 2016. During this time, percent bare soil increased from 11 percent to 73 percent following road surface disturbance from increased traffic and heavy equipment use on East Branch roads. Total rill and plume lengths were on average 1.9 times smaller on rocked roads than native surface roads. Increased bare soil combined with greater precipitation results in greater soil detachment from rain splash and run off from sheetwash (Zeigler et al., 2000; Sugden and Woods, 2007). Ultimately, as soil detachment and transport increase, so do the likelihoods of road-to-stream connectivity (Foltz et al., 2008)

This survey evaluated 6.1 km of active timber harvest road and 2.3 km of inactive timber harvest road between 2014 and 2019. In that time, between one and two percent of active road length and four and nine percent of inactive road length were found clearly connected to the stream network. In Western Oregon, 25 percent of 172 km of forest roads in the Kilchis River watershed were reported connected to streams (Mills, 1997), and in the Sierra Nevada, 30 percent of the 7.7 km of surveyed road length were found connected to the stream network (Stafford, 2011). These values are comparatively higher than the connectivity rates found in this study.

Road-to-stream connectivity was non-existent in Railroad Gulch prior to 2017. However, following timber harvest and an above average precipitation year of 1577 mm, four active road segments and three inactive segments showed connection to the stream

network. Thereafter, active road connectivity decreased to only three road segments while inactive roads increased to six segments. The greater increase from inactive road-to-stream connectivity followed two years of above average precipitation and unmaintained rutting activity from ATV traffic between 2018 and 2019. Lower connectivity on active roads were likely the result of being graded and stormproofed in 2016 following timber harvest which helped stabilized sediment production to road surfaces.

An analysis of this dataset suggest that road design can greatly reduce the connectivity class of a road segment. Ninety percent of the deviance explained by the CART model for predicting decreased connectivity classes was from three primary road design features; 1) lower percent bare soil, 2) decreased slope, and 3) reduced road surface area. These findings are supported by previous studies showing increased frequency of road segment drainage features, increased rock or vegetative armoring, and reduced road surface slopes significantly mitigate runoff generation, erosion rates, and the likelihood of road sediment production and delivery to stream networks (Montgomery, 1994, Ziegler et al., 2000; Coe, 2006; Sosa-Pérez and MacDonald, 2017).

The multiple regression models for predicting annual and storm-based road sediment production were comparable in their input variables. Both models indicated that the product of slope times road segment areas had a significant ($\alpha < 0.01$) positive correlation with sediment production. This parallels other research which suggests that an increase in road segment length does not does not lead to higher sediment production for roads with low slopes, and that the interaction between area and slope is more important

as slope increases (Luce and Black, 1999; Coe, 2006). In addition, sediment production rates from both models were significantly correlated to increasing total rill lengths on the road surface ($\alpha < 0.01$). The positive correlation between increased rill lengths and sediment production are consistent with other studies which have shown that surface runoff can detach and transport more sediment once it is channeled into a rill (Meyer et al., 1975; Loch and Donnellan, 1983; Elliot et al., 2009 Stafford, 2011).

Differences among covariates used in the annual and storm-based models include percent road segment bare soil and grouped storm erosivity events. Sediment production in the multivariate storm-based model showed positive correlation to increased storm erosivity (MJ mm ha^{-1} h^{-1}) with an $\alpha < 0.01$. Consistent with other findings, areas with higher annual erosivities generally have much higher soil detachment from rainsplash erosion and overland flow (Ramos-Scharrón and MacDonald, 2007). The annual-based empirical model suggests that annual sediment production decreases as percent bare soil decreases, and this can be attributed to a reduction in rainsplash erosion and possibly a greater surface roughness which will slow surface runoff velocities (Sosa-Perez and MacDonald, 2017). Coe (2006) found a 16-fold difference in median sediment production rate between roads with rocked surface cover and road segments with native surfaces. The annual and storm-based models developed in the present study were very similar and complemented each other. They also outperformed WEPP: Road.

Both the annual and storm-based empirical models outperformed WEPP: Road in the Bland-Altman concordance analysis with the mean of all differences closer to zero, and observed and measured values in close agreement with all estimates within the 95th

percentile of the upper and lower LOA. Compared to measured values, the annual-based empirical model over predicted sediment production by 28 percent, the storm-based underpredicted by 37 percent, and WEPP: Road underpredicted sediment production values by 95 percent. As measured values increased, WEPP: Road estimates increasingly underestimated sediment production.

The results of this study parallel other findings which suggest that WEPP: Road does not predict road segment sediment production well (Foltz et al., 2008; Elliot et al., 2009; Stafford 2011). One critical source of error in applying WEPP: Road is the lack of covariates in the model that control road segment sediment production. In particular, improvements are needed to address the effects of road surface cover and inter-rill erosion, as these are primary variables driving sediment production rates on forest roads (Elliot et al., 2009; Foltz et al., 2009; Ramos-Scharrón and LaFevor, 2016).

Annual rates of sediment production in Railroad Gulch ranged from 0.0 to 4.8 kg m^{-2} yr^{-1} and appear to be lower compared to literature values. Annual road erosion rates per unit rainfall published since the year 2000 have ranged from 0.2 g m^{-2} mm^{-1} yr^{-1} to 10 g m^{-2} mm^{-1} yr^{-1} (Fu et al., 2010; Sosa-Pérez and MacDonald, 2017). Sediment production rates from individual road segments measured by Barrett and Tomberlin (2006) in the Jackson State Demonstration Forest ranging from 0.5 to 4.0 kg m^{-2} yr^{-1}, were consistent with values measures at this study site, just 250 km to the north.

Future research will be required for natural resource managers to fully understand forest road erosion processes to evaluate and limit the impacts that forest roads can have on the watershed scale. Additional work is needed to define how the magnitude, duration,

frequency, and timing of ATV and timber harvest traffic can impact sediment production and delivery (Meadows, 2008; Welsh, 2008). The similarities between active and inactive road sediment production rates in this study suggest that inactive roads subject to winter and summer ATV use can have similar sediment production rates as road surfaces that have been subject to disturbance from timber harvest. Investigation of surface armoring, such as mulching of road surfaces vs. rock or native surfaces could prove vital to reducing sediment production rates. Furthermore, the importance of understanding models to accurately predict sediment production rates from road surfaces is critical to verifying the range of complex interactions that govern forest road erosion processes.

CONCLUSIONS

This project monitored erosion rates and the production of sediment from actively used and relatively un-trafficked timber harvest roads in Railroad Gulch, a tributary to the lower South Fork Elk River in Humboldt County, California. These issues are of great concern because the associated loading of fine sediment from forest roads into watercourses has been well documented to degrade aquatic ecosystems (Suttle et al., 2004; Foltz et al., 2008). To this end; rainfall, road segment surveys, and road-to-stream connectivity data were collected for 161-202 active road segments and 84 inactive roads segments from 2014 to 2019. Sediment production measurements were collected using silt-fences which were placed on 18 active road segments and nine inactive segments between 2018 to 2019.

Roads constructed and actively used for timber harvest had significantly higher lengths of plume deposition from sheetwash than inactive roads during the same WY's ($\alpha < 0.01$), while rilling between road groups proved limited and non-significant ($\alpha = 0.43$). Sheetwash was dominant due to the cohesive nature of the clay dominated soils which restricted rill and gully formation, as well as, the predominantly low intensity storm events ranging from 0.1-5.0 mm hr^{-1}. Between 2014 and 2019, mean plume lengths below drainages increased from 1.7 m to 5.9 m on actively used roads, while inactive roads increased from 2.2 m to 2.7 m. Rilling on forest roads between 2014 and 2019 was greater on inactive roads, with mean rill lengths expanding from 0.1 m to 2.8 m on active

roads, and from 0.6 m to 5.6 m on inactive roads. When rilling is present on a road segment it will increase plume lengths by a factor of two.

Greater rill and plume lengths were most strongly correlated to increases in percent bare soil, road segment areas, and road slopes. Lack of rill and plume formation on road surfaces occurs most commonly when roads have less than 16 percent bare soil, less than five percent slope, and road segment areas lower than 150 m^2. However, if the road segment has higher than 16 percent bare soil, a slope above eight percent, and a road segment area greater than 83 m^2, then the road segment will likely have plumes greater than 10 m in length. Rill and plume lengths can also be effectively mitigated through the introduction of rock armoring to the road surface.

Inactive road segments had between four and seven percent stream connectivity, whereas active road segments had between one and two percent connectivity following WY's 2017 - 2019. Connectivity from roads to streams were typically surveyed on steeper hillslopes (>20 percent) with shorter distances to streams (<11 m). Forty percent of road segments connected to a stream were associated with rilling. Compared to other studies, Railroad Gulch had very low rates of road-to-stream connectivity and sediment production.

Over the two-year period that silt fences were installed, the mean sediment production rate was 1.1 g m^{-2} mm^{-1} yr^{-1}. Since between one and two percent of active road lengths and between four and nine percent of inactive road lengths were connected between WY 2017 and 2019, an estimated five Mg and nine Mg of sediment would have delivered to the East and West Branch Railroad Gulch, respectively.

Factors controlling sediment production rates in the annual and storm-based multiple regression models suggest that road segments with larger slope*areas, higher percent bare soil, increased rilling on the road surface, and larger grouped storm erosivity events produce greater amounts of sediment. Both models proved to outperform WEPP: Road, which significantly underpredicted sediment production values.

Models to predict road sediment production were variable in their performance when compared to measured values. The annual-based empirical model proved to over predict sediment production by 28 percent with large upper and lower limits in the Bland-Altman diagrams compared to measured values. The storm-based empirical model under estimated sediment production by 37 percent and tended to over predict small events and under predict large events. WEPP: Road was outperformed by both the annual and storm-based empirical models. WEPP: Road underpredicted sediment production values by 95 percent and showed a linear trend in the Bland-Altman diagram indicating that as measured values increase the estimates from WEPP: Road get comparatively smaller.

The results of this study show that both actively used and inactive roads are chronic sources of sediment in the Railroad Gulch watershed. Resource managers can most efficiently reduce the amount of erosion and sediment production from these forest roads by: (1) increasing road surface cover; (2) reducing road slopes to decrease runoff energy; and (3) decrease drainage spacing to reduce road segment areas and hence the amount of runoff from individual segments.

Findings from this study can help improve current models for predicting road sediment production and channel future research. The results can also help resource

managers spotlight effective best management practices for limiting road surface erosion and sediment production from having cumulative effects on the watershed scale.

REFERENCES

Barrett, B., and Tomberlin, D., 2006. Sediment production on forest road surfaces in California's Redwood region: results for HY2006 and HY2007. California Board of Forestry and Fire Protection-Monitoring, Redding, CA, USA.

Bates, D.M., Maechler, M., and Bolker, B., 2012. lme4: Linear mixed-effects models using S4 classes. R package version 0.999999-0.

Brake, D., Molnau, M., and King, J.G., 1997. Sediment transport distances and culvert spacings on logging roads within the Oregon Coast Mountain Range. Presented at the August 28, 1997 Annual International ASAE Meeting, Paper No IM-975018, ASAE, St. Joseph, MI USA.

Brown, E.G., Laird, J., and Pimlott, K., 2018. California Forest Practice Rules. California Department of Forestry, Sacramento, CA, USA.

Cannon, A.R., Cobb, G.W., Hartlaub, B.A., Legler, J.M., Lock, R.H., Moore, T.L., Rossman, A.J., and Witmer, J.A., 2013. STAT2, Building Models for a World of Data, W.H. Freeman, New York, NY, USA.

Coe, D.B., 2006., Sediment Production and Delivery from Forest Roads in the Sierra Nevada, California. MSc thesis. Colorado State University, Fort Collins, CO.

Dunne, T., and Leopold, L., 1978. Water in Environmental Planning. W.H. Freeman and Co., New York, NY, USA.

Elliot, W.J., Foltz, R.B., and Robichaud, P.R., 2009. Recent Findings Related to Measuring and Modeling Forest Road Erosion. Forest Service, Rocky Mountain Research Station 7.

EPA, 2010. What is sediment pollution? United States Environmental Protection Agency. < https://cfpub.epa.gov/npstbx/files/ksmo_sediment.pdf >.

Evenson, R.E., 1959. Geology and Groundwater Features of Eureka Area, Humboldt County, California. USGS Water Supply Paper 1470.

Foltz, R.B., Copeland, N.S., and Elliot, W.J., 2009. Reopening abandoned forest roads in northern Idaho, USA: quantification of runoff, sediment concentration, infiltration, and interrill erosion parameters. J. Environ. Manage. 90: 2542-2550.

Foltz, R.B., Hakjun, R., and William, E.J., 2008. Modeling Changes in Rill Erodibility and Critical Shear Stress on Native Surface Roads. Hydrological Processes 22 (24): 4783.

Fu, B., Newham, L.T., and Ramos-Scharrón, C.E., 2010. A review of surface erosion and sediment delivery models for unsealed roads, Environmental Modelling and Software, 25(1): 1-14.

HRC, 2014. Habitat Conservation Plan. Humboldt Redwood Company. 42-43.

Jones, J.A., Swanson, F.J., Wemple, B.C., and Snyder, K.U., 2000. Effects of Roads on Hydrology, Geomorphology, and Disturbance Patches in Stream Networks. Conservation Biology 14(1): 76–85.

Kolka, R.K., and Smidt, M.F., 2004. Effects of forest road amelioration techniques on soil bulk density, surface runoff, sediment transport, soil moisture, and seedling growth. Forest Ecology and Management. 202: 313-323.

Kwiecien, R., Kopp-Schneider, A., and Blettner, M., 2011. Concordance analysis—part 16 of a series on evaluation of scientific publications. Dtsch Arztebl Int.; 108(30): 515-21.

Loch, R.J., and Donnellan T.E., 1983. Field simulator studies on two clay soils of Darling Downs, Queensland. I. The effect of plot length and tillage orientation on erosion processes and runoff and erosion rates. Australian Journal of Soil Resources. 21:33-46.

Luce, C.H., and Black, T.A., 1999. Sediment production from forest roads in western Oregon. Water Resources Research. 35(8): 2561-2570.

MacDonald, L.H., Coe, D., and Litschert, S., 2003. Assessing cumulative watershed effects in the central Sierra Nevada: Hillslope measurements and catchment-scale modeling. In: Proceedings of the Sierra Nevada Science Symposium: Science for Management and Conservation PSW-GT-193: 149-157.

Meadows, D., Foltz, R., and Geehan, N., 2008. Effects of All-Terrain Vehicles on Forested Lands and Grasslands. Forest Service, National Technology and Development Program.

Megahan, W.F., and Ketcheson, G.L., 1996. Predicting downslope travel of granitic sediments from forest roads in Idaho. Water Resources Bulletin 32(2): 371-382.

Meyer, L.D., Foster, G.R., and Nikolov, S., 1975. Effect of flow rate and canopy cover on rill erosion. Transactions of the American Society of Agricultural Engineering 18: 905-911.

Mills, K., 1997. Forest Roads, Drainage, and Sediment Delivery in the Kilchis River Watershed. Oregon Department of Forestry. Tillamook, OR.

Montgomery, D.R., 1994. Road surface drainage, channel initiation, and slope instability. Water Resources Research. 30(6): 1925-1932.

Mullan, D., Favis-Mortlock, D., and Fealy, R., 2012. Addressing Key Limitations Associated with Modelling Soil Erosion under the Impacts of Future Climate Change. Agricultural and Forest Meteorology 156: 18-30.

NOAA, 2018. "Eureka All Time Records." Accessed January 3, 2018. https://www.wrh.noaa.gov/eka/climate/records.php.

Ramos-Scharrón, C.E., and LaFevor, M.C., 2016. The role of unpaved roads as active source areas of precipitation excess in small watersheds drained by ephemeral streams in the Northeastern Caribbean. J. Hydrology. 53: 168-179.

Ramos-Scharrón, C.E., and MacDonald, L.H., 2007. Development and application of a GIS-based sediment budget model. Journal of Environmental Management. 84: 157-172.

Robichaud, P.R., and Brown, R.E., 2002. Silt fences: an economical technique for measuring hillslope soil erosion. Fort Collins, CO: U.S. Department of Agriculture, Forest Service, Rocky Mountain Research Station.

Schwab, G.O., Fangmeier, D.D., Elliot, W.J., and Frevert, R.K., 1993. Soil and Water Conservation Engineering. John Wiley and Sons, New York.

Sosa-Pérez, G., and MacDonald, L.H., 2017. Reductions in Road Sediment Production and Road-Stream Connectivity from Two Decommissioning Treatments. Forest Ecology and Management. 398: 116-29.

Stafford, A.K., 2011. Sediment Production and Delivery from Hillslopes and Forest Roads in the Southern Sierra Nevada, California. MSc thesis. Colorado State University, Fort Collins, CO.

Sugden, B.D., and Woods, S.W., 2007. Sediment production from forest roads in Western Montana. Journal of the American Water Resources Association 43(1): 193-206.

Suttle, K. B., Mary, P. E., Jonathan, L.M., and McNeely, C. 2004. How Fine Sediment in Riverbeds Impairs Growth and Survival of Juvenile Salmonids. Ecological Applications. 14(4): 969-974.

Therneau, T.M., and Atkinson, E.J., 2019. An Introduction to Recursive Partitioning Using the RPART Routines. Mayo Foundation, 5-57.

Topp, G.C., and Ferré, P.A., 2002. The soil solution phase. In: Jacob, H.D., Topp, G.C. (Eds.), Methods of Soil Analysis: Part 4-Physical Methods. Soil Science Society of America, Inc., Madison, Wisconsin, 417-545.

USDA (United States Department of Agriculture), 2017. RIST (Rainfall Intensity Summarization Tool) http://www.ars.usda.gov/Research/docs.htm?docid= 3251 (accessed 28 December 2018).

Welsh, M.J., 2008. Sediment Production and Delivery from Forest Roads and Off-Highway Vehicle Trails in the Upper South Platte River Watershed, Colorado. MSc thesis. Colorado State University, Fort Collins, CO.

Ziegler, A.D., Sutherland, R.A., and Giambelluca, T.W., 2000. Partitioning total erosion on unpaved roads into splash and hydraulic components: The roles of interstorm surface preparation and dynamic erodibility. Water Resources Research 36(9): 2787-2791.

Ziegler, A.D., Negishi, J.N., Sidle, R.C., Gomi, T., Noguchi, S., and Nik, A.R., 2007. Persistence of road runoff generation in a logged catchment in Peninsular Malaysia. Earth Surf. Proc. Land. 32(13): 1947-1970.

APPENDIX A

Appendix A: Road Summary Field Form

Segment Characteristics		
Road Segment	O	Number
Road Length	M	Tape
Road Width	M	Tape
Road Slope	M	Clinometer
Hillslope	M	Clinometer
Segment Drainage Type	O	Visual
Segment Bare Soil	M/E	Cover Count
Vegetation Coverage	M/E	Cover Count
Fill Slope Percent Bare Soil	E	Cover Count
Fill Slope Thickness	M/E	Tape
Cut Bank Percent Bare Soil	E	Cover Count
Road Design	O	Visual
Road Surface Type	O	Visual
Ditch Present	O	Visual
Ditch Vegetated	O	Visual
Erosion Information		
Erosion Present	O	Visual
Type of Erosion	O	Visual
Drainage feature at end of erosion man made?	O	Visual
Failed Drainage Feature?	O	Visual
Rill Below Drainage		
Rill Length	M	Tape
Average Rill Depth	M	Ruler
Max Rill Depth	M	Ruler
Average Rill Width	M	Tape
Rill Slope	M	Clinometer
Rill Threat to Road	O	Visual
Rill on Road		
Rill Length	M	Tape
Average Rill Depth	M	Ruler
Max Rill Depth	M	Ruler
Average Rill Width	M	Tape
Rill Slope	M	Clinometer
Rill Threat to Road	O	Visual
Plume Below Drainage		
Plume Length	M	Tape
Average Plume Depth	M	Ruler
Max Plume Depth	M	Ruler
Average Plume Width	M	Tape
Plume Roughness	O	Visual

Plume on Road		
Plume Length	M	Tape
Average Plume Depth	M	Ruler
Max Plume Depth	M	Ruler
Average Plume Width	M	Tape
Plume Roughness	O	Visual
Cutbank / Fill Slope Failure		
Length	M	Tape
Height	M	Tape
Max Depth	M	Ruler
Road Length Impacted	M	Tape
Culvert		
Culvert Percent Plugged	E	Visual
Scour at Outlet	O	Visual
Scour Volume	M	Tape
Connectivity		
Connectivity Class (1, 2, 3, 4)	O	Visual
Notes:		
Photo #		

APPENDIX B

Appendix B: Sediment Production Summary

Site	WY	Sediment (kg yr^{-1})	Slope Area	Bare Soil (%)	Total Rill Length (m)	Cut Height (m)	Precipitation (mm)
A008	2018	643	38	0.6	41	2	1035
RR011	2018	376	31	0.2	13	3	1035
RR012	2018	85	21	0.6	13	3	1035
RR013	2018	436	8	0.7	16	2	1035
RR014	2018	0	4	0.55	0	2	1035
RR015	2018	2	6	0.45	0	0	1035
RR040	2018	13	16	0.4	0	2	1035
RR043	2018	83	15	0.4	0	0	1035
RR066	2018	0	10	0.05	0	0	1035
RR085	2018	62	8	0.8	0	3	1035
RR116	2018	2	2	0.95	0	0	1035
RR122	2018	82	11	0.95	7	1	1035
RR123	2018	38	10	0.8	8	1	1035
RR141	2018	436	21	0.97	20	1	1035
RR174	2018	142	21	0.97	0	1	1035
RR175	2018	2	8	0.35	0	1	1035
RR183	2018	368	39	0.94	0	1	1035
RR185	2018	47	11	0.78	0	2	1035
RRC002	2018	0	2	0	0	1	1035
RRC024	2018	549	38	0.6	28	2	1035
RRC025	2018	271	13	0.6	12	2	1035
RRC027	2018	75	11	0.54	7	5	1035
RRC046	2018	9	4	0.4	8	0	1035
RRC049	2018	0	1	0.15	0	0	1035
RRC050	2018	0	1	0.2	0	0	1035
RRC062	2018	0	2	0.1	0	0	1035
RRC078	2018	0	1	0	0	0	1035
RR008	2019	532	38	0.66	57	2	1215
RR011	2019	216	31	0.3	34	3	1215
RR012	2019	4	21	0.2	13	3	1215
RR013	2019	333	8	0.42	16	2	1215

Site	WY	Sediment (kg yr^{-1})	Slope Area	Bare Soil (%)	Total Rill Length (m)	Cut Height (m)	Precipitation (mm)
RR014	2019	0	4	0.2	0	2	1215
RR015	2019	0	6	0.15	0	0	1215
RR040	2019	3	16	0.17	0	2	1215
RR043	2019	44	15	0.37	0	0	1215
RR066	2019	0	10	0	0	0	1215
RR085	2019	45	8	0.21	18	3	1215
RR116	2019	1	2	0.2	0	0	1215
RR122	2019	99	11	0.48	7	1	1215
RR123	2019	17	10	0.4	8	1	1215
RR141	2019	419	21	0.66	23	1	1215
RR174	2019	112	21	0.39	0	1	1215
RR175	2019	2	8	0.13	0	1	1215
RR183	2019	550	39	0.49	23	1	1215
RR185	2019	23	11	0.22	0	2	1215
RRC002	2019	0	2	0	0	1	1215
RRC024	2019	559	38	0.33	37	2	1215
RRC025	2019	335	13	0.29	73	2	1215
RRC028	2019	393	10	0.34	66	9	1215
RRC046	2019	7	4	0.11	11	0	1215
RRC049	2019	0	1	0.06	0	0	1215
RRC050	2019	0	1	0.1	2	0	1215
RRC062	2019	0	2	0.08	0	0	1215
RRC078	2019	0	1	0	0	0	1215

APPENDIX C

Appendix C: WEPP: Road Model Output

Site	Design	Surface, traffic	Rd grad (%)	Rd length (m)	Rd width (m)	Fill grad (%)	Fill length (m)	Buff grad (%)	Average annual rain runoff (in)	Average annual sediment leaving road (kg)
RR008	Outsloped, rutted	native low	20	37	5	20	37	37.5	5.9	21.8
RR011	Outsloped, rutted	native low	30	20	5	15	20	40	4	10.9
RR012	Outsloped, rutted	native low	20	23	5	30	23	40	4.9	10.4
RR013	Outsloped, rutted	native low	10	18	5	5	18	32.5	3.1	4.1
RR014	Outsloped, unrutted	native low	5	14	6	28	14	17.5	2.1	2.3
RR015	Outsloped, unrutted	native low	5	26	5	10	26	15	2.1	3.6
RR040	Outsloped, unrutted	native low	10	34	5	10	34	30	3.1	6.8
RR043	Outsloped, unrutted	native low	10	27	5	45	27	20	3	5.9
RR066	Outsloped, unrutted	native low	5	38	5	30	38	15	2.9	5.4
RR085	Outsloped, unrutted	native low	9	15	5	31	15	30	3	3.2
RR116	Outsloped, unrutted	native low	3	15	5	23	15	20	1.9	1.8
RR122	Outsloped, rutted	native low	8	25	5	28	25	17.5	3.6	5.4
RR123	Outsloped, rutted	native low	5	40	5	20	40	17.5	4.7	7.3
RR141	Outsloped, rutted	native low	15	27	5	0.3	1	25	3.1	9.1
RR174	Outsloped, unrutted	native low	10	41	5	0.3	1	20	1.8	8.2
RR175	Outsloped, unrutted	native low	5	32	5	0.3	1	5	1.3	4.5
RR183	Outsloped, unrutted	native low	18	42	5	0.3	1	35	3.4	14.5
RR185	Outsloped, unrutted	native low	15	15	5	28	15	65	4.2	5.0
RR008	Outsloped, rutted	native low	20	37	5	20	37	37.5	5.9	21.8

Site	Design	Surface, traffic	Rd grad (%)	Rd length (m)	Rd width (m)	Fill grad (%)	Fill length (m)	Buff grad (%)	Average annual rain runoff (in)	Average annual sediment leaving road (kg)
RR011	Outsloped, rutted	native low	30	20	5	15	20	40	4	10.9
RR012	Outsloped, rutted	native low	20	23	5	30	23	40	4.9	10.4
RR013	Outsloped, rutted	native low	10	18	5	5	18	32.5	3.1	4.1
RR014	Outsloped, unrutted	native low	5	14	6	28	14	17.5	2.1	2.3
RR015	Outsloped, unrutted	native low	5	26	5	10	26	15	2.1	3.6
RR040	Outsloped, unrutted	native low	10	34	5	10	34	30	3.1	6.8
RR043	Outsloped, unrutted	native low	10	27	5	45	27	20	3	5.9
RR066	Outsloped, unrutted	native low	5	38	5	30	38	15	2.9	5.4
RR085	Outsloped, rutted	native low	9	15	5	31	15	30	3.2	3.2
RR116	Outsloped, unrutted	native low	3	15	5	23	15	20	1.9	1.8
RR122	Outsloped, rutted	native low	8	25	5	28	25	17.5	3.6	5.4
RR123	Outsloped, rutted	native low	5	40	5	20	40	17.5	4.7	7.3
RR141	Outsloped, rutted	native low	15	27	5	0.3	27	25	3.2	8.6
RR174	Outsloped, unrutted	native low	10	41	5	0.3	41	20	2.5	8.2
RR175	Outsloped, unrutted	native low	5	32	5	0.3	32	5	1.9	4.5
RR183	Outsloped, rutted	native low	18	42	5	0.3	42	35	4.4	20.9
RR185	Outsloped, unrutted	native low	15	15	5	28	15	65	4.2	5.0
RRC002	Outsloped, unrutted	native low	9	14	2	0.3	1	5	1.1	0.9
RRC024	Outsloped, rutted	native low	22	33	5	0.3	1	62.5	4.2	18.1
RRC025	Outsloped, rutted	native low	18	16	5	0.3	1	27.5	2.3	5.0
RRC027	Outsloped, rutted	native low	20	29	2	0.3	1	70	3.8	5.4
RRC046	Outsloped, rutted	native low	10	21	2	0.3	1	32.5	3	1.8

Site	Design	Surface, traffic	Rd grad (%)	Rd length (m)	Rd width (m)	Fill grad (%)	Fill length (m)	Buff grad (%)	Average annual rain runoff (in)	Average annual sediment leaving road (kg)
RRC049	Outsloped, unrutted	native low	2	38	2	0.3	1	22.5	0.9	1.8
RRC050	Outsloped, unrutted	native low	4	20	2	0.3	1	20	0.9	1.4
RRC062	Outsloped, unrutted	native low	6	20	2	0.3	1	20	1	1.4
RRC078	Outsloped, unrutted	native low	5	16	2	0.3	1	25	1	0.9
RRC002	Outsloped, unrutted	native low	9	14	2	0.3	1	5	1.1	0.9
RRC024	Outsloped, rutted	native low	22	33	5	0.3	1	62.5	4.2	18.1
RRC025	Outsloped, rutted	native low	18	16	5	0.3	1	27.5	2.3	5.0
RRC028	Outsloped, rutted	native low	20	87	2	0.3	1	30	8	34.0
RRC046	Outsloped, rutted	native low	10	21	2	0.3	1	32.5	3	1.8
RRC049	Outsloped, rutted	native low	2	38	2	0.3	1	22.5	3.6	1.8
RRC050	Outsloped, rutted	native low	4	20	2	0.3	1	20	2.2	0.9
RRC062	Outsloped, unrutted	native low	6	20	2	0.3	1	20	1	1.4
RRC078	Outsloped, unrutted	native low	5	16	2	0.3	1	25	1	0.9